

DTIC COPY

REPORT DOCUMENTATION PAGE				Form Approved OMB No. 0704-01-0188	
<p>The public reporting burden for this collection of information is estimated to average 1 hour per response, including the time for reviewing instructions, searching existing data sources, gathering and maintaining the data needed, and completing and reviewing the collection of information. Send comments regarding this burden estimate or any other aspect of this collection of information, including suggestions for reducing the burden to Department of Defense, Washington Headquarters Services Directorate for Information Operations and Reports (0704-0188), 1215 Jefferson Davis Highway, Suite 1204, Arlington VA 22202-4302. Respondents should be aware that notwithstanding any other provision of law, no person shall be subject to any penalty for failing to comply with a collection of information if it does not display a currently valid OMB control number.</p> <p><b>PLEASE DO NOT RETURN YOUR FORM TO THE ABOVE ADDRESS.</b></p>					
1. REPORT DATE (DD-MM-YYYY) 06-01-2010		2. REPORT TYPE REPRINT		3. DATES COVERED (From - To)	
4. TITLE AND SUBTITLE Contrasting O/X-mode heater effects on O-mode sounding echo and the generation of magnetic pulsations				5a. CONTRACT NUMBER	
				5b. GRANT NUMBER	
				5c. PROGRAM ELEMENT NUMBER 62601F	
6. AUTHORS Spencer Kuo* Wei-Te Cheng* Arnold Snyder** Paul Kossey James Battis				5d. PROJECT NUMBER 1010	
				5e. TASK NUMBER HR	
				5f. WORK UNIT NUMBER A2	
7. PERFORMING ORGANIZATION NAME(S) AND ADDRESS(ES) Air Force Research Laboratory /RVBX 29 Randolph Road Hanscom AFB, MA 01731-3010				8. PERFORMING ORGANIZATION REPORT NUMBER AFRL-RV-HA-TR-2010-1001	
9. SPONSORING/MONITORING AGENCY NAME(S) AND ADDRESS(ES)				10. SPONSOR/MONITOR'S ACRONYM(S) AFRL/RVBXI	
				11. SPONSOR/MONITOR'S REPORT	
12. DISTRIBUTION/AVAILABILITY STATEMENT Approved for Public Release; distribution unlimited.				20100201214	
13. SUPPLEMENTARY NOTES Reprinted from <i>Geophysical Research Letters</i> , Vol. 37, L01101, doi:10.1029/2009GL041471, 2010 ©2010, American Geophysical Union *Polytechnic Institute, New York University, Brooklyn, NY **NorthWest Research Associates, Stockton Springs, ME					
14. ABSTRACT The effects on the ionosphere of powerful O-mode and X-mode pump waves, modulated 3 minutes on and 1 minute off, were explored. The experiments were monitored using the digisonde and magnetometer located at the HAARP facility. The results show that the virtual heights of the O-mode sounding echoes shifted down/up as the O/X mode heater was turned on; the ionosphere also moved downward/upward accordingly. Enhanced spread-f was also observed in O-mode heater-on periods. Heater-induced magnetic pulsation was observed. Its intensity increased progressively in the heater on/off sequence and X-mode heater was more effective than O-mode heater in the generation of magnetic pulsation. In the last X-mode heater-on period, when the magnetic pulsation reached the highest level, pc 3 pulsations, with increasing intensity, were also observed.					
15. SUBJECT TERMS HAARP      Ionospheric heating      X-mode      O-mode      Pulsations					
16. SECURITY CLASSIFICATION OF:			17. LIMITATION OF ABSTRACT	18. NUMBER OF PAGES	19a. NAME OF RESPONSIBLE PERSON
a. REPORT	b. ABSTRACT	c. THIS PAGE			James Battis
UNCL	UNCL	UNCL	UNL		19b. TELEPHONE NUMBER (Include area code)

## Contrasting O/X-mode heater effects on O-mode sounding echo and the generation of magnetic pulsations

Spencer Kuo,<sup>1</sup> Wei-Te Cheng,<sup>1</sup> Arnold Snyder,<sup>2</sup> Paul Kossey,<sup>3</sup> and James Battis<sup>3</sup>

Received 22 October 2009; revised 30 November 2009; accepted 2 December 2009; published 6 January 2010.

[1] The effects on the ionosphere of powerful O-mode and X-mode HF pump waves, modulated 3 minutes on and 1 minute off, were explored. The experiments were monitored using the digisonde and magnetometer located at the HAARP facility. The results show that the virtual heights of the O-mode sounding echoes shifted down/up as the O/X mode heater was turned on; the ionosphere also moved downward/upward accordingly. Enhanced spread-F was also observed in O-mode heater-on periods. Heater-induced magnetic pulsation was observed. Its intensity increased progressively in the heater on/off sequence and X-mode heater was more effective than O-mode heater in the generation of magnetic pulsation. In the last X-mode heater-on period, when the magnetic pulsation reached the highest level, pc 3 pulsations, with increasing intensity were also observed. **Citation:** Kuo, S., W.-T. Cheng, A. Snyder, P. Kossey, and J. Battis (2010), Contrasting O/X-mode heater effects on O-mode sounding echo and the generation of magnetic pulsations, *Geophys. Res. Lett.*, 37, L01101, doi:10.1029/2009GL041471.

### 1. Introduction

[2] A major facility for conducting ionospheric heating experiments is available in Gakona, Alaska, as part of the High Frequency Active Auroral Research Program (HAARP) [Kossey *et al.*, 1999]. HAARP HF transmitting system consists of 180 crossed dipole antennas arranged as a rectangular, planar array. Each antenna element radiates circularly polarized wave up to 20 kW in the frequency band from 2.8 MHz to 10 MHz, over which the antenna gain increases from 15 dB to 30 dB with increasing radiating frequency. It is anticipated that HF heating of the ionosphere will make a significant impact by both collision and anomalous heating processes.

[3] In heating experiments, the HF heater wave is normally transmitted in the X-mode (left-hand (LH) circular polarization), or in the O-mode (right-hand (RH) circular polarization), with the heater frequency  $\omega_0 < \omega_{pe}$ , the plasma frequency of the F peak. These heating waves impact the ionosphere through different processes. One process is to excite parametric instabilities. However, this requires that the heating wave be accessible to the spatial regions where the parametric coupling conditions can be

matched [Fejer, 1979; Stenflo, 1985]. Consequently, the region directly impacted by instabilities is limited to close to the reflection layer of the heater. In the present work, an experiment was conducted to explore the effects of O/X-mode heating on a broad region of the ionosphere by examining digisonde and magnetometer records. ULF waves can be produced by the HF heater via filamentation instability [Kuo and Lee, 1983] or other dynamo processes [Papadopoulos and Chang, 1985]. Filamentation instability [Kuo and Schmidt, 1983] simultaneously generates large-scale field-aligned density irregularities (FAIs) as has been observed in a recent HAARP heating experiment [Kuo *et al.*, 2009]. Hence, the magnetometer records may be used to infer the presence of heater-induced large-scale FAIs in addition to the scintillation method used by others [Frey *et al.*, 1984; Secan *et al.*, 1997].

### 2. Experimental Observations

[4] On March 18, 2009 from UTC 20:45 to UTC 21:08, from UTC 21:35 to UTC 22:08, and from UTC 22:11 to UTC 22:50, using the HAARP transmitter facility at Gakona, AK, at full power (3.6 MW) experiments were conducted with HF heater waves of 3.2 MHz directed along the geomagnetic zenith. From 20:45 to 21:08, O-mode and X-mode heating modulated with 3 minutes on and 1 minute off were transmitted alternatively. The rectangular modulation wave had 6 cycles in the 24 minutes experimental period. In the next two time periods, only X-mode pump waves were transmitted. From 21:35 to 22:08, the heater was modulated with 3 minutes on and 3 minutes off for 6 cycles, and then the modulation was changed to 3 minutes on and 1 minute off for 10 cycles in the period from 22:11 to 22:50.

[5] The experiments were monitored by the HAARP digisonde and magnetometer. Because the HF heating wave is in the frequency band of the digisonde, it can be recorded by the digisonde receiver as a false return with much stronger intensity that degrades the image resolution of the true returns. To avoid this occurrence, the ionogram is blanked in a frequency band around the heater frequency. Specifically for these examples, the returns in the band approximately from 3 to 3.4 will be blank. The exact ionogram bandwidth around the heater frequency is determined by a combination of ionosonde functions such as automatic gain control, signal threshold determination, and the signal detection threshold of the receiver.

#### 2.1. Heater Induced Virtual Height Variation

[6] The ionograms in the frequency bands of 2.5 to 2.9 MHz and 3.55 to 3.95 MHz were then examined to extract evidence of generating large-scale FAIs by the HF

<sup>1</sup>Polytechnic Institute, New York University, Brooklyn, New York, USA.

<sup>2</sup>NorthWest Research Associates, Stockton Springs, Maine, USA.

<sup>3</sup>Space Vehicles Directorate, Air Force Research Laboratory, Hanscom AFB, Massachusetts, USA.



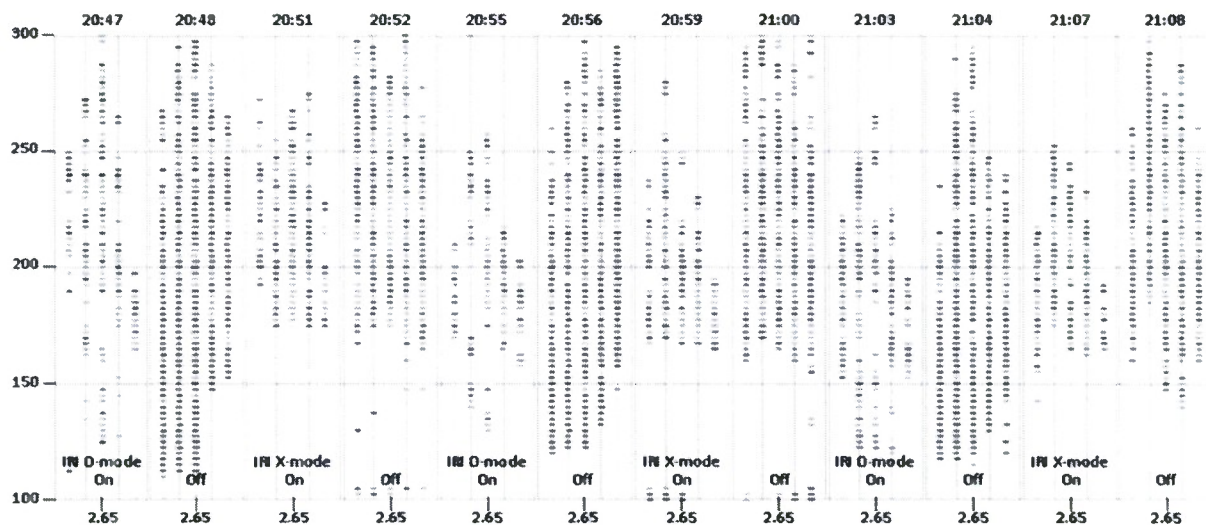


**Figure 1.** Sequence of ionograms of O-mode sounding echoes in the frequency band of 2.52 to 2.73 MHz, recorded from 20:47 to 21:08 with 3.2 MHz O/X-mode HF pump waves, modulated with 3 minutes on and 1 minute off, transmitted alternatively.

heater. The digisonde was run in a relatively fast mode that produced ionograms during the heater on and off periods for purposes of comparison.

[7] We first examined the ionograms recorded in the first experimental period from 20:45 to 21:08. The effect of the HF heating on the virtual heights of the O-mode sounding echoes in the frequency band of 2.52 to 2.73 MHz was explored by directly comparing the ionograms. The results of six consecutive heater-on/off sequences, presented in Figure 1, show that the virtual heights of the echo shift down (or up) as the O (or X) mode heating is turned on. The recording of the ionogram was started at the beginning of

a minute, and the time span for a complete scan from 1 to 6 MHz was about 37 seconds. Thus, echoes in the 2.52 to 2.73 MHz band of the off period ionograms were recorded at about 11 to 13 seconds after the heater was turned off. As seen in Figure 1, although the virtual heights of the echoes in each off period ionogram, are not much different from those in the preceding on period ionogram, which suggests that the ionospheric recovery time is longer than 13 seconds, the change of the color code of the echoes has a significant meaning. In the plots, red and blue echoes represent negative and positive Doppler shifted vertical O-mode echoes, i.e., echoes from up-moving and down-moving ionosphere. In

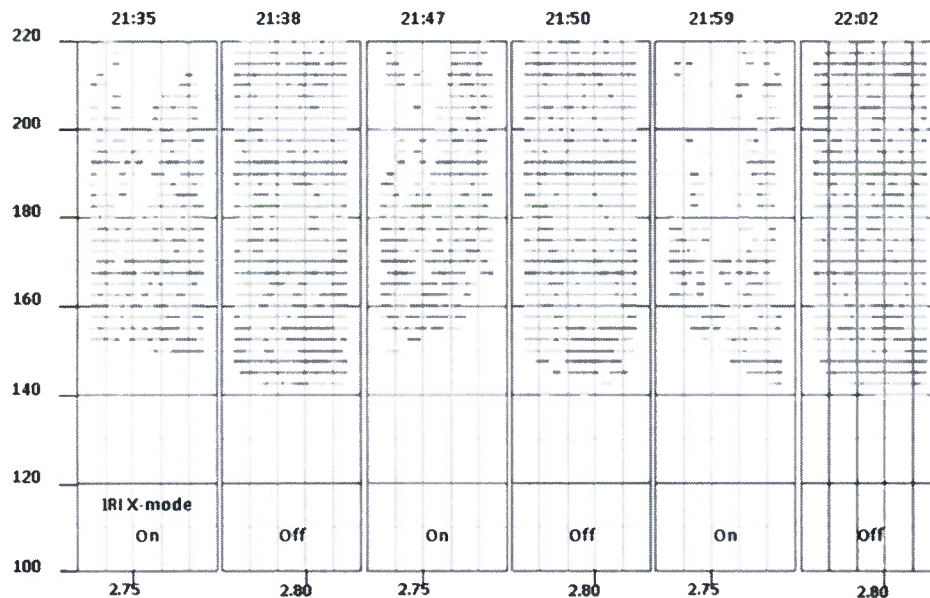


**Figure 2.** Sequence of ionograms of O-mode sounding echoes in the frequency band of 2.68 to 2.87 MHz, recorded from 21:35 to 22:02 with 3.2 MHz X-mode HF pump wave, modulated with 3 minutes on and 3 minutes off.

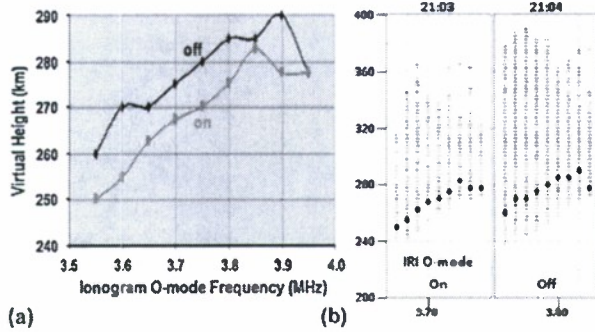


**Figure 3.** Effect of O-mode HF pump wave on the (a) virtual height and (b) intensity of O-mode sounding echo.

one cycle with O-mode heater on/off and then X-mode heater on/off, the color change of the majority of the echoes, from blue to red and then red to blue, indicates that O-mode heater moves the ionosphere down and X-mode heater moves it up; and in the off period, ionosphere moves up (or down) to recover the prior down (or up) shift by the O (or X) mode heating. Figure 1 also shows that O-mode heater caused an artificial spread-F, which persisted even after the heater was turned off for more than the 13 seconds corresponding to the time delay in transmitting sounding pulses in the frequency band of 2.52 to 2.73 MHz.

[8] The fact that X-mode heater moves the ionosphere up can be seen clearly during the second experimental period from 21:35 to 22:08. Three sets of on/off ionograms in the frequency band of 2.68 to 2.87 MHz are presented in Figure 2 to show the consistent effect of the X-mode heater on lifting the ionosphere.

[9] This contrasting effect of O and X mode heating on the virtual heights of the O-mode sounding echoes also appears in the frequency band of 3.55 to 3.95 MHz of the ionograms. This is exemplified by showing two cases analyzed from two sets of heater on/off ionograms, which were recorded in 20:03/20:04 and 21:35/21:38. The frequency dependencies of the virtual heights of the highest amplitude O-mode sounding echoes in the two cases, corresponding to O and X-mode heater on/off, are plotted in Figures 3a and 4a, respectively. As shown, the virtual heights of the echoes were also downshifted by the O-mode heater (Figure 3a) and upshifted by the X-mode heater (Figure 4a). This contrasting trend is also identified visually from the corresponding ionograms presented in Figures 3b and 4b, in which the point of the intensity peak at each sounding frequency is marked by a black dot. It is noted that every echo in the ionograms of Figures 1–4 is plotted with the same size rectangle regardless of its amplitude.

## 2.2. Excitation of Geomagnetic Micropulsation

[10] The induced magnetic field variation was monitored by the fluxgate magnetometer located at Gakona, AK. The 1 sec resolution data from UTC 20:45 to UTC 21:08 were averaged for over 10 sec periods providing 18 average values in each heater on period (180 sec) and 6 average values in each heater off period (60 sec). These average values contain both the background magnetic field as well as any variation caused by changes of the electrojet. A four point algorithm is

developed to extract the heater-induced component from the average data. This algorithm extrapolates heater-independent magnetic field in a heater-on period by using the heater-off values at the two ends of the heater-on period. Each point is extrapolated by the three adjacent points, one in the front and two in the back. The front point is unknown, thus the extrapolation is done from both directions simultaneously. Consider one on period and its two adjacent off periods; taking only 2 average values in each heater off period and label the 22 average values ( $2 + 18 + 2$ ) in these three periods (off-on-off) by  $A_j$ ,  $j = 1, 2, \dots, 22$ , where  $(A_1, A_2)$  and  $(A_{21}, A_{22})$  are the average values in the front and back off periods. Let  $A_j = A_j^0 + \Delta B_j$ , where  $\Delta B_j$ ,  $j = 1, 2, \dots, 22$ , are the average magnetic field produced by the heater in each 10 sec slot, where  $(\Delta B_1, \Delta B_2)$  and  $(\Delta B_{21}, \Delta B_{22})$  are zero. Using the relations, deduced approximately from the Runge-Kutta algorithm [Conte and de Boor, 1972] by representing the slope functions in the algorithm in terms of finite differences between points,  $A_n \cong A_{n+1} - \frac{1}{3}A_{n+2} + \frac{1}{3}A_{n-1} \cong A_{n-1} - \frac{1}{3}A_{n-2} + \frac{1}{3}A_{n+1}$ , yield

$$\begin{aligned} \Delta B_n = A_n - (1/80)\{[n(22-n) + (n-1)(21-n)]A_2 \\ - [(n-2)(22-n) + (n-3)(21-n)]A_1\} \\ - (1/80)\{[(n-1)(23-n) + (n-2)(22-n)]A_{21} \\ - [(n-1)(21-n) + (n-2)(20-n)]A_{22}\} \end{aligned}$$

(1)

for  $n = 3, 4, \dots, 19, 20$ ;

[11] We then use (1) to process the averaged magnetometer data. The results reveal the evolution of the 10 sec average magnetic field induced by the heater in one on-period.

[12] The results of  $\Delta B_H$  (pink curve),  $\Delta B_D$  (blue), and  $\Delta B_Z$  (green) in three directions (H, D, and Z), from UTC 20:45 to 21:09, are presented in Figure 5. As shown, the magnetic field fluctuation induced by the X-mode heater is larger than that induced by the O-mode heater; the intensity and oscillatory features of the induced magnetic fields, in both heating-mode cases, develop with the duration of the heating cycles. The peak intensity of  $\Delta B_D$  reaches 1.5 nT and 2 nT in the last O-mode (21:01 to 04) and X-mode (21:05 to 08) heating cycle. In the  $\Delta B_H$  and  $\Delta B_Z$  components, the development of oscillatory feature is more pronounced. Furthermore,  $\Delta B_H$  in the last X-mode heating cycle has evolved into *pc* 3 pulsations with increasing inten-

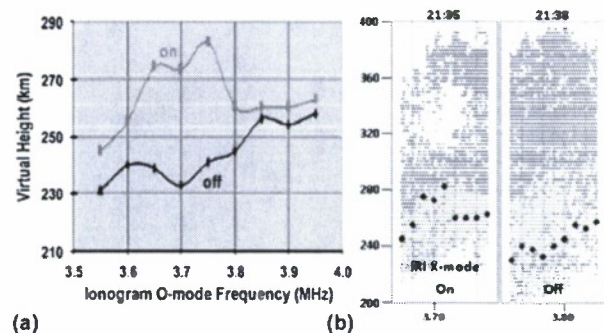


**Figure 4.** Effect of X-mode HF pump wave on the (a) virtual height and (b) intensity of O-mode sounding echo.



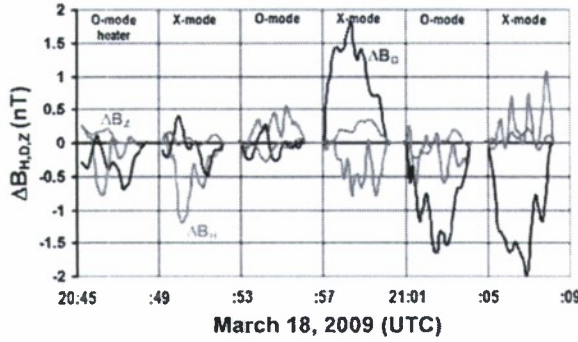


**Figure 5.** H (pink), D (blue), and Z (green) components of the magnetic field fluctuation induced by the HF pump wave.

sity. The polarities of  $\Delta B_H$  and  $\Delta B_D$  in X-mode heating cycles are basically opposite to each other; on the other hand,  $\Delta B_H$  and  $\Delta B_D$  have the same polarity in O-mode heating cycles. These contrasting differences in the induced magnetic fluctuations suggest that the density irregularities generated by the O and X-mode heaters are quite different in the characteristic features including polarization, scale size, and magnitude.

### 3. Discussion

[13] The O-mode heater is reflected at a height near the electron plasma resonance layer, where the electron plasma frequency  $\omega_{pO} = \omega_0$  and is located higher than the upper hybrid resonance layer  $\omega_{pU} = (\omega_0^2 - \Omega_e^2)^{1/2}$ . Therefore, O-mode heating wave is accessible to the spatial regions where many parametric coupling conditions can be matched [Fejer, 1979; Stensflo, 1985]. Parametric instabilities convert HF heating wave to plasma waves which heat the ionosphere locally near the HF reflection height. Such anomalous heating forms a local heat source which transmits heat downward through heat conduction along the magnetic field. Consequently, the ionosphere moves downward and a thermal instability [Kuo and Djuth, 1988] is also excited to generate large-scale FAIs which enhance spread-F as seen in Figure 1.

[14] On the other hand, the X-mode heater will be reflected at a height having a plasma frequency of  $\omega_{pX} = [\omega_0(\omega_0 - \Omega_e)]^{1/2}$  that is below the electron plasma resonance layer as well as below the upper hybrid resonance layer. Although the X-mode heater cannot effectively introduce a similar anomalous heating in the F-region it heats the ionosphere through the collision process more effectively than does the O-mode heating. The quiver speeds  $|V_{q\pm}|$  of electrons in the O/X-mode heating wave electric field  $E$  are given by  $|V_{q\pm}| = |eE/m|[(\omega_0 \pm \Omega_e)^2 + \nu^2]^{-1/2}$ , where  $\Omega_e$  and  $\nu$  are the electron cyclotron and collision frequencies. Thus the ratio  $\xi$  of the X to O-mode collision heating rates is obtained to be  $\xi = [(\omega_0 + \Omega_e)^2 + \nu^2]/[(\omega_0 - \Omega_e)^2 + \nu^2] \cong (\omega_0 + \Omega_e)^2/(\omega_0 - \Omega_e)^2 \gg 1$ . The collision heating process is non-local and moves the ionosphere upward.

[15] The electron thermal pressure force, arising from the differential ohmic heating on electrons [Gurevich, 1976; Fejer, 1979] by the combined wave electric field of the HF heater and the excited high frequency sidebands, pushes electrons to form large-scale FAIs, which in turn break up

the HF pump wave by filamentation instability [Kuo and Schmidt, 1983]. The electron thermal pressure force  $F_{H1}$  also gives rise to an  $F_H \times B_0$  drift motion in the electron fluid and induces a net electron drift current flowing perpendicular to both the background magnetic field  $B_0$  and the spatial variation direction of the produced density irregularities. Therefore, magnetic field pulsations are excited simultaneously with large scale density irregularities by the filamentation instability [Kuo and Lee, 1983; Lee and Kuo, 1985]. Pc 5 pulsations have been observed in Tromsø heating experiments [Stubbe and Kopka, 1981] and ULF waves have been observed by Chang *et al.* [2008] in HAARP heating experiments. However, it is noted that the present experiment was conducted around local solar noon during a geomagnetic quiet time, thus the generation of magnetic pulsations is electrojet independent. The collision heating by the X-mode heating is more effectively than that by the O-mode heating and it explains the observation in Figure 5 that the heater-induced magnetic pulsations are more intense in X-mode heater-on periods. The heater was modulated with 3 minutes on and 1 minute off so the generation of Pc 3 pulsations in the X-mode heater-on period was not directly related to the modulation period. Pc 3 pulsations could be generated by the current pulsations in closing the loops of currents driven by heater-induced thermal pressure force.

[16] **Acknowledgments.** We are grateful to Bodo Reinisch and his team members Dima Paznukhov and Ivan Galkin for fruitful discussions. This work was supported by the High Frequency Active Auroral Research Program (HAARP), AFRL at Hanscom AFB, MA, and by the Office of Naval Research, grant ONR-N00014-05-1-0109. Part of the financial support was arranged through NorthWest Research Associates, Inc.

### References

- Chang, C., J. Labenski, H. Shroff, I. Doxas, D. Papadopoulos, G. Milikh, and M. Parrot (2008), Ground and satellite observations of ULF waves artificially produced by HAARP, *Eos Trans. AGU*, 89(53), Fall Meet. Suppl., Abstract SA42A-07.
- Conte, S. D., and C. de Boor (1972), *Elementary Numerical Analysis*, McGraw-Hill, New York.
- Fejer, J. A. (1979), Ionospheric modification and parametric instabilities, *Rev. Geophys.*, 17, 135, doi:10.1029/RG017i001p00135.
- Frey, A., P. Stubbe, and H. Kopka (1984), First experimental evidence of HF produced electron density irregularities in the polar ionosphere: Diagnosed by UHF radio star scintillations, *Geophys. Res. Lett.*, 11, 523, doi:10.1029/GL011i005p00523.
- Gurevich, V. A. (1976), Nonlinear phenomena in the ionosphere, *Radio-phys. Quantum Electron.*, Engl. Transl., 19, 595, doi:10.1007/BF01043546.
- Kossey, P., J. Heckscher, H. Carlson, and E. Kennedy (1999), HAARP: High Frequency Active Auroral Research Program, *J. Arct. Res. U. S.*, 1, 1.
- Kuo, S. P., and F. T. Djuth (1988), A thermal instability for the spread F echoes from the HF-heated ionosphere, *Geophys. Res. Lett.*, 15, 1345, doi:10.1029/GL015i012p01345.
- Kuo, S. P., and M. C. Lee (1983), Earth magnetic field fluctuations produced by filamentation instabilities of electromagnetic heater waves, *Geophys. Res. Lett.*, 10, 979, doi:10.1029/GL010i010p00979.
- Kuo, S. P., and G. Schmidt (1983), Filamentation instability in magneto plasmas, *Phys. Fluids*, 26, 2529, doi:10.1063/1.864442.
- Kuo, S. P., W.-T. Cheng, J. A. Cohen, R. Pradipta, M. C. Lee, S. S. Kuo, and A. Snyder (2009), Simultaneous generation of large-scale density irregularities and geomagnetic pulsations via filamentation instability, *Geophys. Res. Lett.*, 36, L09107, doi:10.1029/2009GL037942.
- Lee, M. C., and S. P. Kuo (1985), Simultaneous generation of large-scale geomagnetic field fluctuations and plasma density irregularities by powerful radio waves, *Radio Sci.*, 20, 539, doi:10.1029/RS020i003p00539.
- Papadopoulos, K., and C. L. Chang (1985), Generation of ELF/ULF waves in the ionosphere by dynamo processes, *Geophys. Res. Lett.*, 12, 279, doi:10.1029/GL012i005p00279.
- Secan, J. A., R. M. Bussey, E. J. Fremouw, and S. Basu (1997), High-latitude upgrade to the wideband ionospheric scintillation model, *Radio Sci.*, 32, 1567, doi:10.1029/97RS00453.

- Stenflo, L. (1985), Parametric excitation of collisional modes in the high-latitude ionosphere, *J. Geophys. Res.*, 90, 5355, doi:10.1029/JA090iA06p05355.
- Stubbe, P., and H. Kopka (1981), Generation of *Pc* 5 pulsations by polar electrojet modulation: First experimental evidence, *J. Geophys. Res.*, 86, 1606, doi:10.1029/JA086iA03p01606.
- 
- J. Battis and P. Kossey, Space Vehicles Directorate, Air Force Research Laboratory, 29 Randolph Rd., Hanscom AFB, MA 01731, USA.
- W.-T. Cheng and S. Kuo, Polytechnic Institute, New York University, 6 MetroTech Ctr., Brooklyn, NY 11201, USA.
- A. Snyder, NorthWest Research Associates, PO Box 530, Stockton Springs, ME 04981, USA.